Electronic Supplementary Material (ESI) for RSC Advances.

Hydrophilicity and Surface Charge Modulation of $Ti_3C_2T_x$ MXene Based Membranes for Water Desalination

Laxmi Pandey,[a] *Wentao Liang*[a] *Armin VahidMohammadi*[d], *Teng Zhang*[d], *Yury Gogotsi*[d] *and Meni Wanunu*[*a,b,c]

[a] Department of Physics, Northeastern University, Boston, MA 02115, USA

[b] Department of Bioengineering, Northeastern University, Boston, MA 02115, USA

[c] Department of Chemistry and Chemical Biology, Northeastern University, Boston, MA 02115, USA

[d] A.J. Drexel Nanomaterials Institute and Department of Materials Science and Engineering, Drexel University, Philadelphia, PA 19104, USA

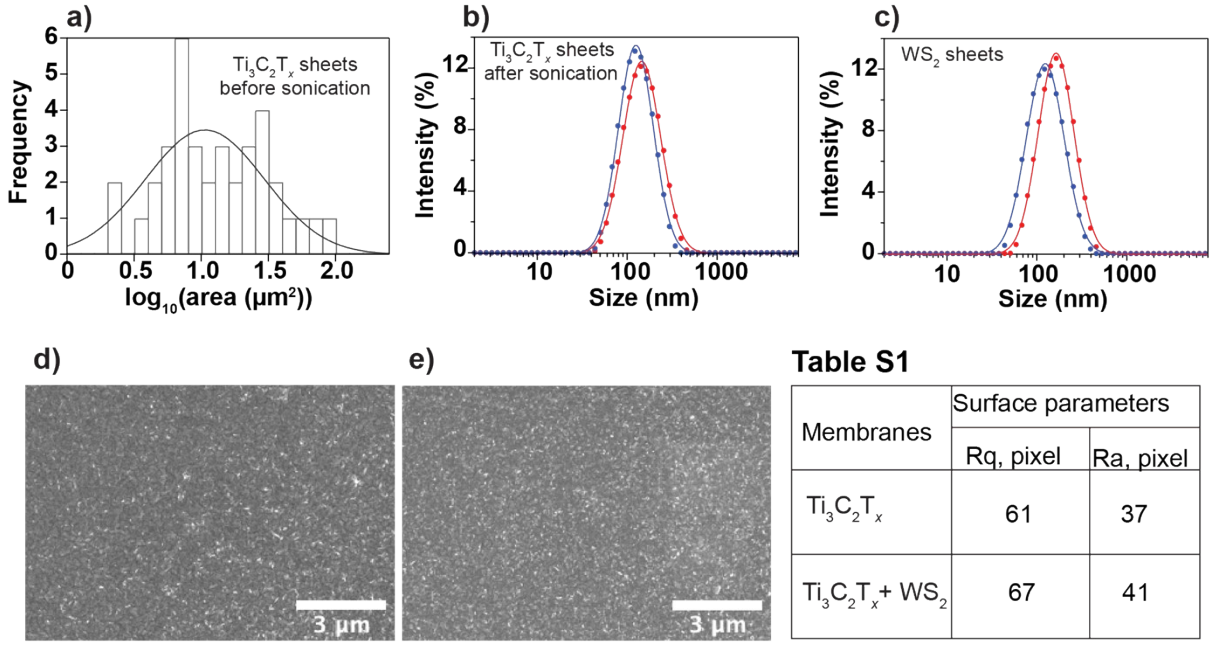

Table S1

Membranes	Surface parameters	
	Rq, pixel	Ra, pixel
$Ti_3C_2T_x$	61	37
$Ti_3C_2T_x$+ WS_2	67	41

Figure S1: Nanosheets and membrane surfaces characterization: a) area of $Ti_3C_2T_x$ (before sonication) measured with ImageJ from three different AFM images; b) and c) size of $Ti_3C_2T_x$ nanosheets (after 1.5 hours of ultrasonic probe sonication with Hielscher UP100H at 60% power) measured with Zetasizer Nano ZS and WS_2 measured with Zetasizer Nano ZS respectively, two curves are shown here to compare the batch-to-batch nanosheet size differences. d) and e) SEM surface images of $Ti_3C_2T_x$ and $Ti_3C_2T_x$ + WS_2 membranes, respectively. Table S1 reports the surface parameters of membranes obtained by analyzing SEM images (d and c) using ImageJ software.

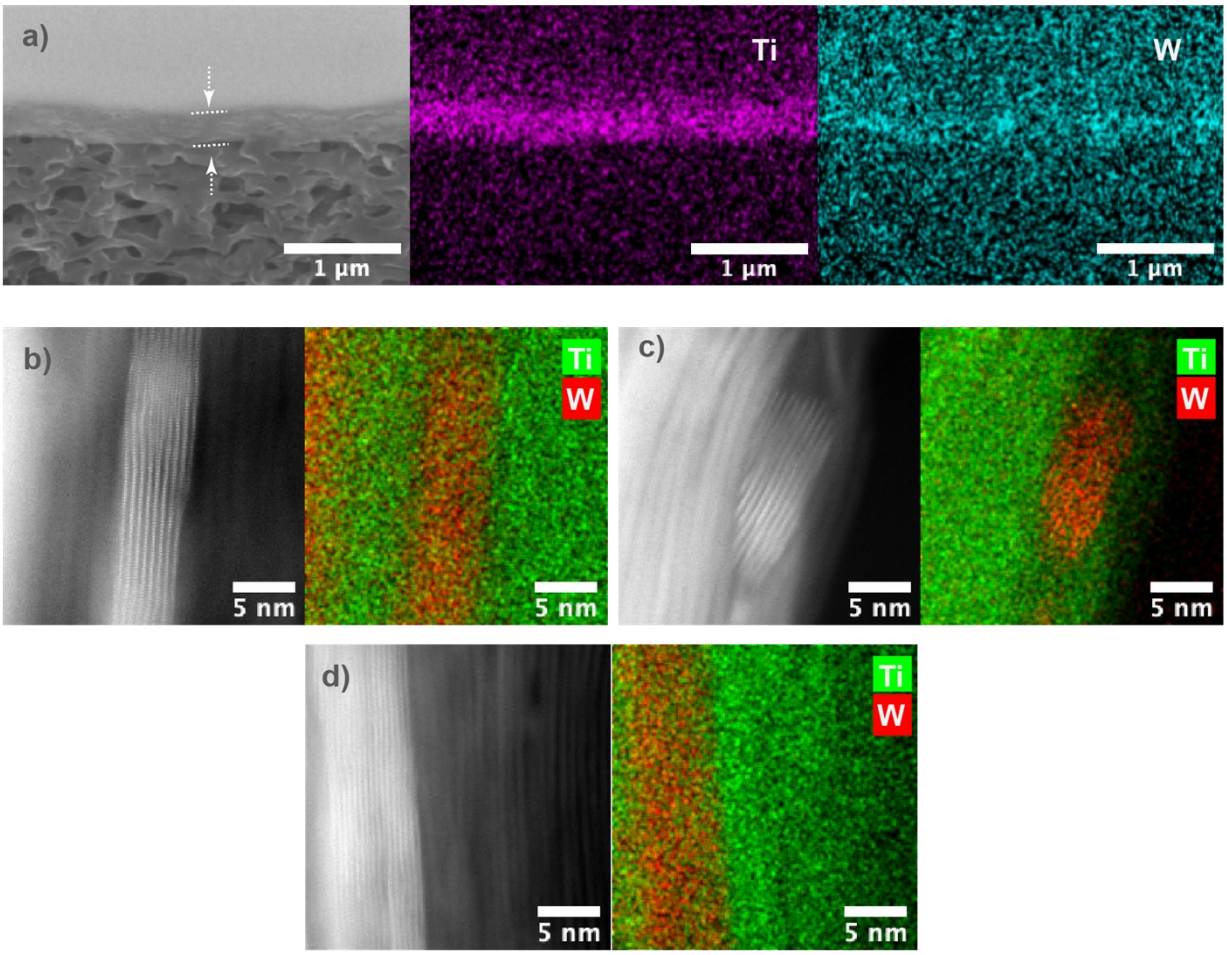

Figure S2: Cross-section characterization of a $Ti_3C_2T_x$ + WS_2 composite membrane: a) SEM image and false-color EDX elemental maps for Ti (purple) and W (light blue). b-d) HAADF-STEM image along with false-color EDX elemental maps for Ti (green) and W (red) of different parts of the membrane.

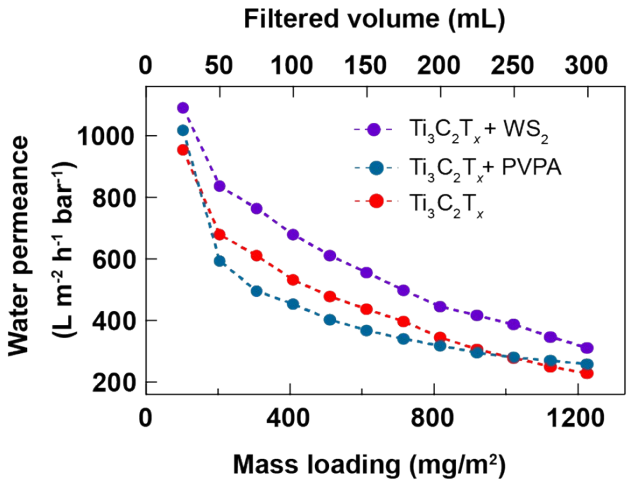

Figure S3: Comparison of water permeance of different membranes based on mass loading. 3 mL of solution containing 0.2 mg/mL of nanosheets was first diluted to 300 mL and vacuum filtered on PES substrate. To prepare MXene + WS_2 suspension, 2 mL of 0.2 mg/mL of MXene was mixed with 1 mL of 0.2 mg/mL of WS_2.

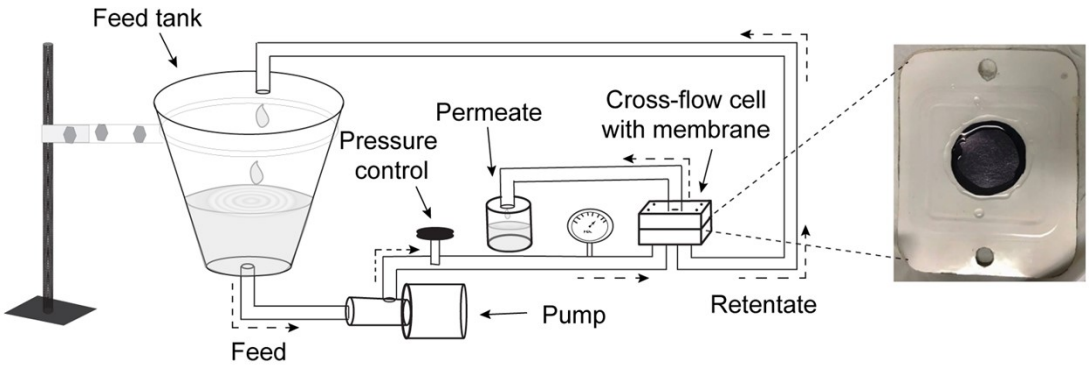

Figure S4: Schematic illustration of the cross-flow system. The membrane to be tested is fitted in the cross-flow cell, and the feed tank is filled with a salt solution pressurized by the pump. Dashed arrows show the direction of feed and permeate flow.

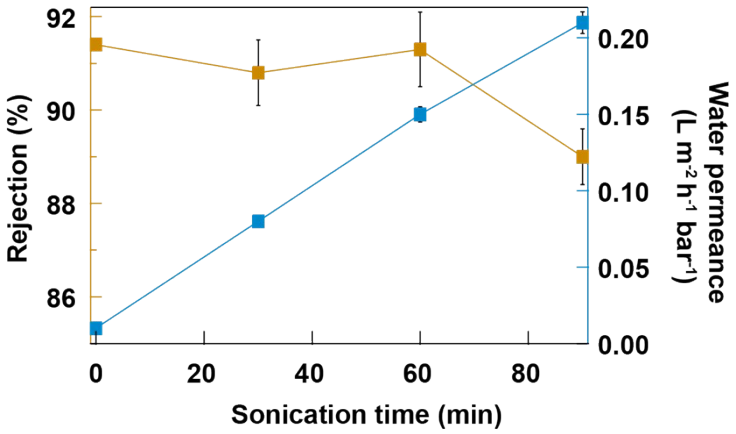

Figure S5: Performance of $Ti_3C_2T_x$ lamellar membrane in the cross-flow system as a function of $Ti_3C_2T_x$ nanosheet sonication time. Longer sonication times lead to a reduction in the mean nano-capillary length by reducing nanosheet size, which helps to increase water permeance. The feed solution was 0.02 M Na_2SO_4 in these experiments.

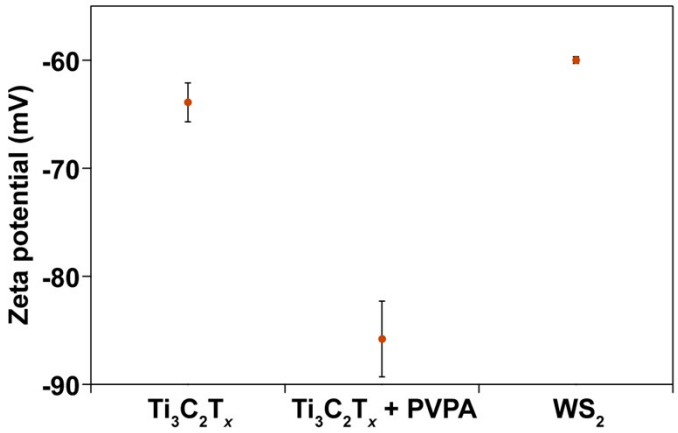

Figure S6: Comparison of zeta potential of $Ti_3C_2T_x$ (90 min sonicated nanosheets), WS_2, and $Ti_3C_2T_x$ + PVPA dispersion in an aqueous solution. The concentration of nanosheets in each dispersion was 0.1 mg/mL. $Ti_3C_2T_x$ + PVPA dispersion was prepared by heating 1% of PVPA with 0.2 mg/mL of $Ti_3C_2T_x$ at 90°C for about 20 min. For pH adjustment, HCl and NaOH were added to the dispersion dropwise.

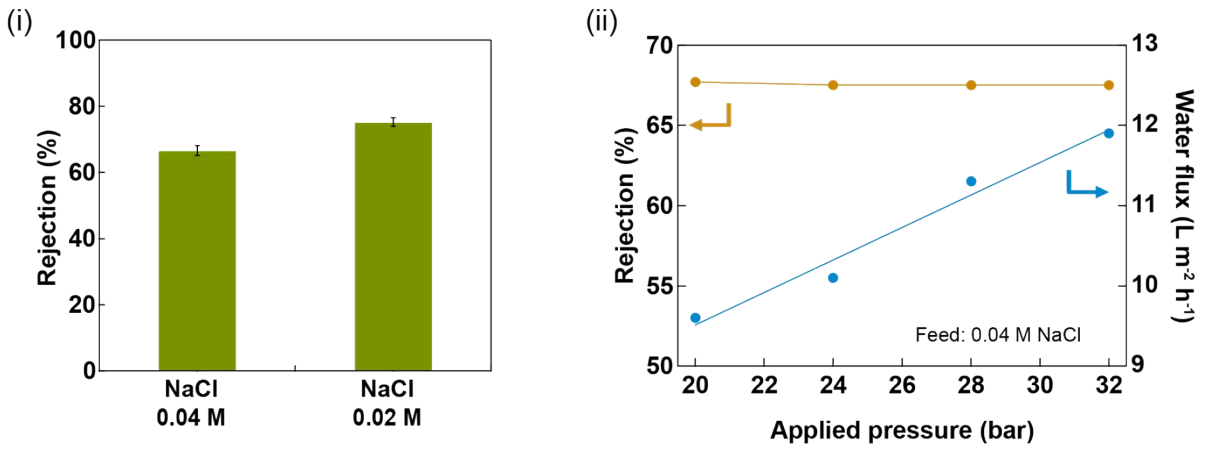

Figure S7: (i) Concentration-dependent , (ii) Pressure-dependent performance of MXene + WS_2 membrane. The mass ratio of MXene and WS_2 was 2:1 in these membranes. For concentration dependent performace, applied pressure was 20 bar.

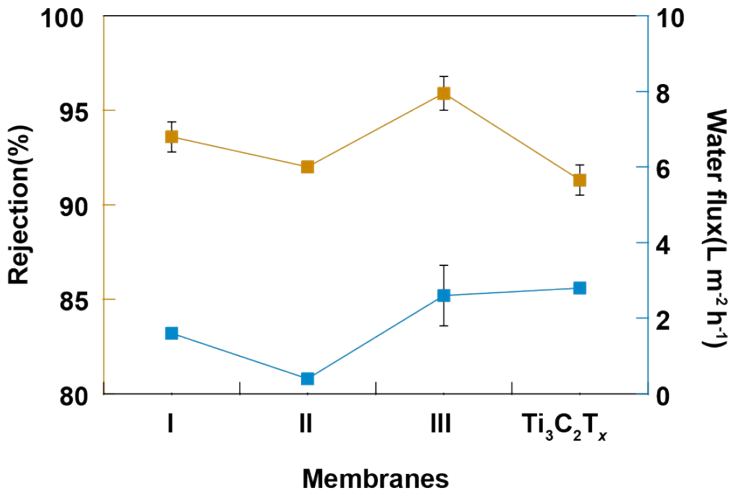

Figure S8: Comparison of $Ti_3C_2T_x$ + PVPA prepared under the different conditions with $Ti_3C_2T_x$ - only membrane. For optimization purposes, PVPA was mixed with $Ti_3C_2T_x$ dispersion and prepared the membrane in 3 cases: for type I membrane, the membrane was prepared by mixing 1% PVPA with 0.05mg/mL of $Ti_3C_2T_x$ dispersion, and the membrane was dried at room temperature; for type II membrane, the membrane was prepared by mixing 1% PVPA with 0.05mg/mL of $Ti_3C_2T_x$ dispersion and the membrane was dried at 80°C; for type III membrane, the dispersion (1% PVPA with 0.1mg/mL) was heated at 80°C to 90°C for about 20 min, and the membrane was prepared and dried at room temperature. Feed, 0.02 M Na_2SO_4, was pressurized at 20 bar in these experiments.

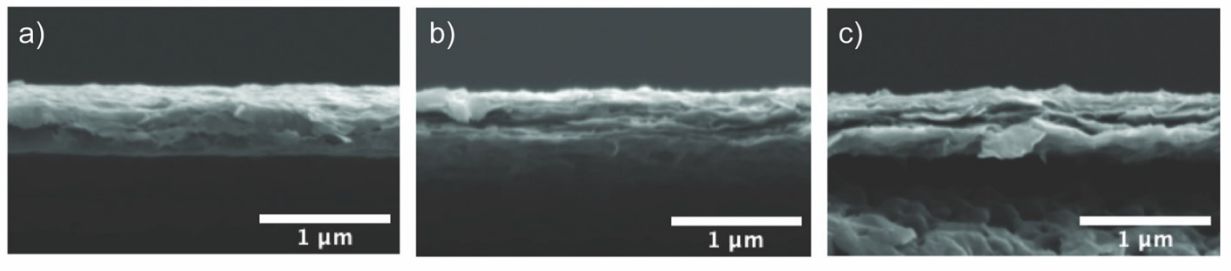

Figure S9: Thickness comparison of $Ti_3C_2T_x$ based membranes; Cross-section SEM image of a) $Ti_3C_2T_x$ membrane, b) $Ti_3C_2T_x$ + WS_2 membrane, and c) $Ti_3C_2T_x$ + PVPA membrane, respectively. These membranes were 0.5 µm thick.

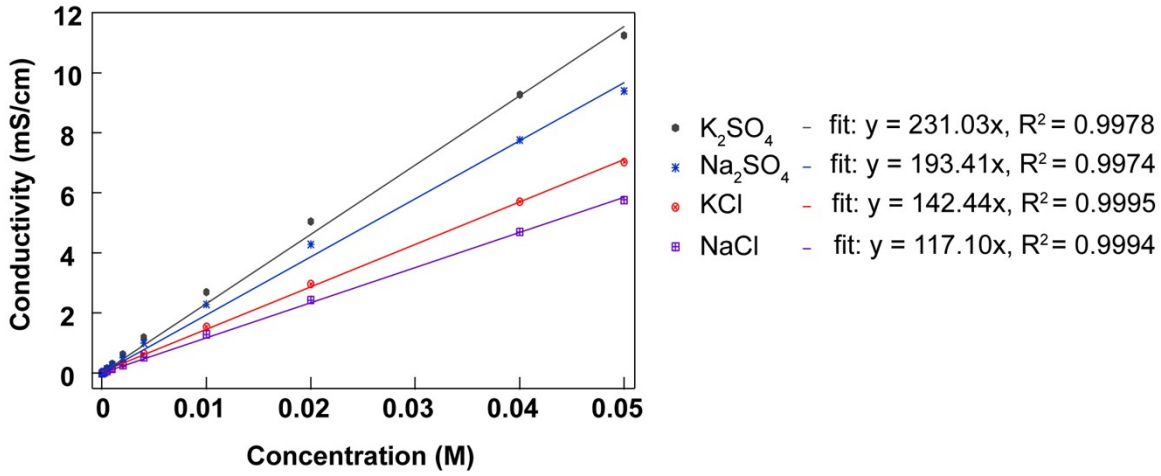

Figure S10: Concentration vs. conductivity graph for different salts. The conductivity of DI was minimal (~1 µS/cm), so line fits were forced to pass through the origin.

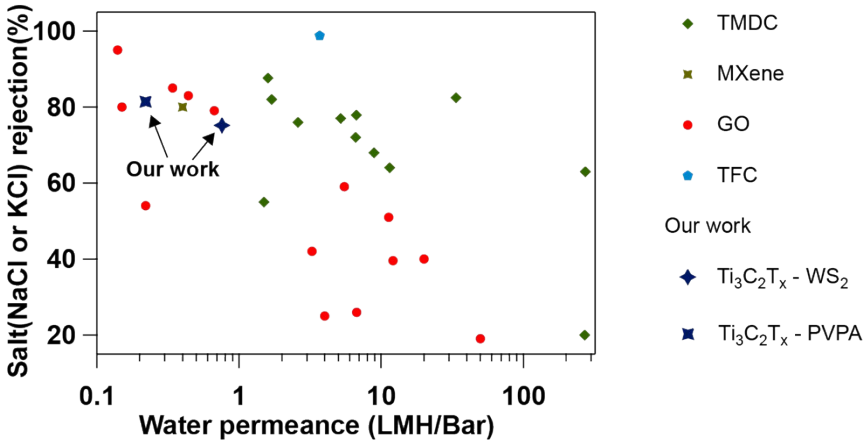

Figure S11: Comparison of the performance of $Ti_3C_2T_x$ - based membranes in this work with other literature reports for GO[1-6], MXene[7], TMDC[8-11] and TFC[12] membranes.

References:

1 Yang, Q. *et al.* Ultrathin graphene-based membrane with precise molecular sieving and ultrafast solvent permeation. *Nature Materials* **16**, 1198-1202 (2017). https://doi.org:10.1038/nmat5025

2 Guan, K. *et al.* Nanochannel-confined charge repulsion of ions in a reduced graphene oxide membrane. *Journal of Materials Chemistry A* **8**, 25880-25889 (2020). https://doi.org:10.1039/D0TA08881A

3 Hu, M. & Mi, B. Enabling Graphene Oxide Nanosheets as Water Separation Membranes. *Environmental Science & Technology* **47**, 3715-3723 (2013). https://doi.org:10.1021/es400571g

4 Han, Y., Xu, Z. & Gao, C. Ultrathin Graphene Nanofiltration Membrane for Water Purification. *Advanced Functional Materials* **23**, 3693-3700 (2013). https://doi.org:https://doi.org/10.1002/adfm.201202601

5 Han, Y., Jiang, Y. & Gao, C. High-Flux Graphene Oxide Nanofiltration Membrane Intercalated by Carbon Nanotubes. *ACS Applied Materials & Interfaces* **7**, 8147-8155 (2015). https://doi.org:10.1021/acsami.5b00986

6 Morelos-Gomez, A. *et al.* Effective NaCl and dye rejection of hybrid graphene oxide/graphene layered membranes. *Nature Nanotechnology* **12**, 1083-1088 (2017). https://doi.org:10.1038/nnano.2017.160

7 Zhu, J. *et al.* Precisely Tunable Ion Sieving with an Al13–$Ti_3C_2T_x$ Lamellar Membrane by Controlling Interlayer Spacing. *ACS Nano* **14**, 15306-15316 (2020). https://doi.org:10.1021/acsnano.0c05649

8 Ries, L. *et al.* Enhanced sieving from exfoliated MoS_2 membranes via covalent functionalization. *Nature Materials* **18**, 1112-1117 (2019). https://doi.org:10.1038/s41563-019-0464-7

9 Mei, L. *et al.* Simultaneous electrochemical exfoliation and covalent functionalization of MoS_2 membrane for ion sieving. *Advanced Materials* **n/a**, 2201416 (2022). https://doi.org:https://doi.org/10.1002/adma.202201416

10 Sapkota, B. *et al.* High permeability sub-nanometre sieve composite MoS_2 membranes. *Nature Communications* **11**, 2747 (2020). https://doi.org:10.1038/s41467-020-16577-y

11 Hoenig, E. *et al.* Controlling the Structure of MoS_2 Membranes via Covalent Functionalization with Molecular Spacers. *Nano Letters* **20**, 7844-7851 (2020). https://doi.org:10.1021/acs.nanolett.0c02114

12 Kadhom, M. & Deng, B. Synthesis of high-performance thin film composite (TFC) membranes by controlling the preparation conditions: Technical notes. *Journal of Water Process Engineering* **30**, 100542 (2019). https://doi.org:https://doi.org/10.1016/j.jwpe.2017.12.011